1-8-2022

The Source of Auroral Omegas

Heidi K. Nykyri
Embry-Riddle Aeronautical University, nykyrik@erau.edu

J.M. Weygand
University of California Los Angeles

Mostafa El-Alaoui
Catholic University of America

Scholarly Commons Citation

Weygand, J. M., El-Alaoui, M., & Nykyri, H. K. (2022). The source of auroral omegas. Journal of Geophysical Research: Space Physics, 127, e2021JA029908. https://doi. org/10.1029/2021JA029908

JGR Space Physics

RESEARCH ARTICLE
10.1029/2021JA029908

Key Points:

- We show several examples of hemispherically conjugate auroral omegas, which demonstrates their source is within the magnetotail
- Conjugate ASIs of omegas and spacecraft magnetic field and particle data show that ~80% of events are correlated with high speed flows
- Only 10% of the events appear to occur during high speed dawnward flows, which could be associated with a Kelvin-Helmholtz instability

Supporting Information:

Supporting Information may be found in the online version of this article.

Correspondence to:

J. M. Weygand,
jweygand@igpp.ucla.edu

Citation:

Weygand, J. M., El-Alaoui, M., & Nykyri, H. K. (2022). The source of auroral omegas. *Journal of Geophysical Research: Space Physics*, *127*, e2021JA029908. https://doi.org/10.1029/2021JA029908

Received 23 AUG 2021
Accepted 20 DEC 2021

Author Contributions:

Formal analysis: H. K. Nykyri
Funding acquisition: M. El-Alaoui
Investigation: M. El-Alaoui, H. K. Nykyri
Methodology: H. K. Nykyri
Supervision: H. K. Nykyri
Visualization: M. El-Alaoui
Writing – original draft: M. El-Alaoui, H. K. Nykyri
Writing – review & editing: M. El-Alaoui, H. K. Nykyri

The Source of Auroral Omegas

J. M. Weygand[1,2], M. El-Alaoui[3,4], and H. K. Nykyri[5]

[1]Institute of Geophysics and Planetary Physics, University of California Los Angeles, Los Angeles, CA, USA, [2]Department of Earth, Planetary, and Space Sciences, University of California Los Angeles, Los Angeles, CA, USA, [3]NASA Goddard Space Flight Center, Greenbelt, MD, USA, [4]Catholic University of America, Washington, DC, USA, [5]Physical Sciences Department College, Daytona College of Arts & Sciences, Embry Riddle Aeronautical University, Daytona Beach, FL, USA

Abstract The auroral wave-like structures called "omega bands" appear within the post-midnight sector auroral oval with shapes resembling the Greek letter omega, and are typically associated with the recovery phase of substorms. Prior work and MHD simulations suggest both high speed earthward flows and post-midnight flow shears are possible omega band source mechanisms. However, what produces omega bands is not well understood. It is most likely that the paucity of concurrent magnetospheric data has limited our ability to understand fully the mechanism responsible for the generation of the omega bands. We have identified about 263 auroral omegas in seven different THEMIS all sky cameras (ASCs) over a 10 year period. A fraction appear to form from north-south streamers, but some appear to form from east-west auroral arcs. Fifty-one of the 263 Ω also have conjugate or near conjugate THEMIS and GOES spacecraft data. There is evidence in about 80% of these events that high speed earthward flows have occurred prior to or at about the same time as the auroral omega observation. This evidence consists of high speed earthward flows, magnetic field dipolarizations, particle injections into the inner magnetosphere, and auroral streamers. 11 events also show plasma flow data azimuthally along the inner magnetosphere, but for six of these events the V_y component is inconsistent with the auroral omega direction of motion. Of the remaining five events, four have V_y flow shear events but also show evidence of magnetic field dipolarizations, particle injections into the inner magnetosphere, and auroral streamers. Our observations suggest high speed earthward flows are more likely to be the source of auroral omega bands.

1. Introduction

The auroral wave-like structures called "omega bands" was first described by Akasofu and Kimball (1964), however, the mechanism by which auroral omegas are produced is still not known. They are typically associated with the expansion and recovery phase of magnetic substorms (Partamies et al., 2017; Vanhamäki et al., 2009) and correlated with Ps6 magnetic pulsations (Saito, 1978). Omega bands can consist of several nearly equally spaced structures that propagate from west to east with a speed of 400–2,000 m/s (Mravlag et al., 1991; Opgenoorth et al., 1983; Yamamoto et al., 1993) consistent with the average $\vec{E} \times \vec{B}$ plasma drift velocity (André & Baumjohann, 1982). However, a single auroral omega is not uncommon and the omega bands are not always equally spaced (Partamies et al., 2017; Weygand et al., 2015). Auroral observations of omega bands and Ps6 pulsations have been recorded in both hemispheres on the same day, which suggests they may be conjugate in both hemispheres and the source mechanism may be in the magnetotail, but the observations were not at the exact same time (Mravlag et al., 1991).

The Ps6 magnetic pulsations observed in all three components of ground-based magnetometer measurements demonstrate that a three-dimensional current system is present within the ionosphere for auroral omegas. A significant amount of work has been done to understand the three-dimensional ionospheric current system of omegas (Amm, 1996; André & Baumjohann, 1982; Gustafsson et al., 1981; Kawasaki & Rostoker, 1979; Lühr & Schlegel, 1994; Opgenoorth et al., 1983). Those studies have found that the brightest edges of the omega bands lie near the interface between the region 1 and region 2 current system in the morning sector, which indicates they are associated with the earthward edge of the plasma sheet.

Several of studies have employed magnetic field models to field line trace the auroral omegas from the ionosphere to the equatorial magnetospheric location (Pulkkinen et al., 1991; Tagirov, 1993; Wild et al., 2011). With Tsyganenko's 1989 (T89) magnetic field model (Tsyganenko, 1989), Pulkkinen et al. (1991) showed that the omega bands observed on 25 March 1986 mapped to 6 to 13 R_E down the magnetotail. Tagirov (1993) demonstrated, also

with the T89 model, that the auroral omega bands observed on 9–10 April 9–10 1986 occurred 5–6 R_E down the magnetotail. The auroral omega bands viewed 28 September 2009 over Iceland with the Tjörnes all sky camera (ASC) were believed to be conjugate with the Cluster spacecraft located at ~8 R_E down the magnetotail (Wild et al., 2011) based on the magnetic field line tracing completed with the Tsyganenko 2001 (T01) model (Tsyganenko, 2002a, 2002b). Weygand et al. (2015) has also mapped the omega bands between 6 and 18 R_E with the Tsyganenko's 1996 (T96) and T01 models.

Ground based measurements of auroral omega bands are relatively common; however, spacecraft measurements of the magnetospheric signature of omega bands are rare. The extent of spacecraft measurements are obtained with auroral imagers such as Polar, IMAGE, and Viking (Henderson et al., 1998, 2002; Opgenoorth et al., 1994; Henderson, 2009, 2012; Amm et al., 2005). As far as we are aware, only the Wild et al. (2011) and Partamies et al. (2017) studies provide spacecraft observations in the tail on or near field lines conjugate to auroral omegas. The study of Wild et al. (2011) did not demonstrate a one-to-one correlation between the in situ plasma or magnetic observations and auroral structures, but did display enhanced Alfvénic Poynting flux and transient bursts of electron differential energy flux with dispersed energy signatures throughout the event when spacecraft foot points were magnetic field line mapped to the region of the omega bands. Partamies et al. (2017) did a statistical study of hundreds of auroral omegas and examined a few events with spacecraft data. One event had Geotail observations of a high speed flow in the magnetotail tail on 1998 at 2215 UT that mapped few degrees to the west of the Abisko ASC at 68.36° GLat and 18.82° EGLONG. Shortly after the end of the high speed flow measurements an auroral omega entered the view of the ASC from the west. This single event suggests that the high speed flows are the source of the auroral omega. However, Partamies et al. (2017) examined one other event with Geotail observations that mapped a couple of degrees to the northwest of the auroral omega. In this event no high speed flows or other significant features in the plasma flow or magnetic field were observed.

Weygand et al. (2015) performed a detailed study of five Ω band intervals with the total of 26 Ω structures over the THEMIS ASC network on 9 March 2008. The auroral omegas were observed in the post-midnight sector at the boundary between region 1 and region 2 currents and 5 auroral omegas were observed to evolve from auroral streamers. High speed plasma sheet flows were observed by the THEMIS spacecraft prior to some of the ionospheric auroral omega images. Also recorded were dipolarizations in the GOES magnetic field data at about the same local time. The most likely generation mechanism for the observed auroral omega bands was believed to be the plasma sheet high speed flows. Optical observations of the development of the 5 Ω after north-south streamers supported their conclusion. However, 10 of 26 auroral omegas evolved without any association with auroral streamers, which suggests that another generation mechanism is possible.

At this time we do not yet understand the generation mechanism for auroral omegas. This gap in our ability to understand why the auroral omegas occur is most likely due to the lack of conjugate or near conjugate magnetospheric data. However, several generation mechanisms, which are discussed in Amm et al. (2005), have been proposed. The most widely accepted generation mechanisms are (a) that omega bands form as a direct consequence of north-south streamer events (Roux et al., 1991; Henderson, 2009, 2012), where north-south streamers are the ionospheric projection of earthward flow burst in the plasma sheet. These earthward flow bursts are the result of magnetic field reconnection in the tail (Nishimura et al., 2011). (b) Or auroral omegas form through the structuring of magnetic vorticity and field-aligned currents in the ionosphere by the Kelvin-Helmholtz instability driven by flow shears at the inner edge of the plasma sheet (Janhunen & Huuskonen, 1993; Rostoker & Samson, 1984). However, it has been suggested that the electrostatic KH instability in the magnetosphere can be suppressed by the effect of ionospheric (Pedersen) current closure (e.g., Keskinen et al., 1988; Yamamoto, 2009). Another magnetotail generation mechanism is one discussed throughout Yamamoto et al. (1993, 1997, 2008, 2009, 2011) who believes auroral omegas are the result of a hybrid Kelvin-Helmholtz/Rayleigh-Taylor (KH/RT) instability in the plasma sheet. Yamamoto (2011) states that the hybrid KH/RT waves primarily in the magnetotail causes earthward directed bursty bulk flows, leading to the formation of north-south streamer auroras, and the auroral omegas are end result of those streamers.

The high speed flow/auroral streamer mechanism predicts that spacecraft in the magnetotail should record magnetic field dipolarizations, high speed earthward flows and particle enhancements at the earthward edge of the plasma sheet and/or geosynchronous orbit. At the ionosphere, auroral omegas would appear to form from north south streamers. Such observations can be made with the THEMIS and GOES spacecraft. The flow shear mechanism predicts flow shears at around 6–13 R_E within the magnetotail, oscillations near the shear in the radial

Table 1
Locations of the Magnetometer Stations Used in This Study

Station	Station code	GLat.	GLong.	Mlat.	Mlong.
Athabasca	ATHA	54.7°	246.7°	61.7°	307.2°
Fort Simpson	FSIM	61.7°	238.8°	67.2°	294.4°
For Smith	FSMI	60.0°	248.1°	67.3°	307.0°
Gillam	GILL	56.4°	265.3°	66.0°	333.2°
Kuujjuaq	KUUJ	58.1°	291.6°	66.6°	13.4°
Sanikiluaq	SNKQ	56.5°	280.8°	66.1°	357.2°
Whitehorse	WHIT	61.0°	224.8°	63.6°	279.6°

Note. In the first two columns are the station name followed by the station code. In the third and fourth columns are the geographic latitude and longitude and in the last two columns are the magnetic latitude and longitude.

component of the magnetic field, and the region 1 currents should exceed the region 2 currents prior to the flow shear but the two current systems are nearly equal during the auroral omega bands (Yamamoto, 2009; 2011). The flow shear mechanism could potentially be observed by the THEMIS spacecraft mission. In the shear flow and KH/RT mechanisms, the auroral omegas are observed to form in the ionosphere at the boundary of Region 1 and Region 2 currents.

This study presents evidence toward identifying the source of auroral omega bands. In the Data section, spacecraft and instrumentation employed in this study are discussed and, in the Observations section, we investigate several events in detail that support the various source mechanisms. In the Discussion we provide statistical results and model results as well as we interpret the MHD model results in relation to the ASC and spacecraft observations.

2. Data

The data for our study come from four sources: the THEMIS ASCs, the THEMIS spacecraft magnetic field and particle data, the GOES spacecraft magnetic field and particle data, and the DMSP SUSSI images.

To identify the auroral omegas we used the THEMIS all sky images (ASIs). The white light ASIs are recorded every three seconds from an array of ground-based observatories with overlapping field of views spread over Canada, Alaska, and Greenland. More details on the ASIs and the ASC geographic locations are available in Donovan et al. (2006) and Mende et al. (2008).

The THEMIS spacecraft mission consists of five identical spacecraft, initially placed in elliptical orbits with different apogees that align every 4 days (Angelopoulos, 2008). Each spacecraft has five instruments but we examined data from the ElectroStatic Analyzer (ESA), Solid State Telescopes (SST), and the triaxial FluxGate Magnetometer (FGM). The combined ESA and SST data provide fundamental plasma parameters such as density and velocity vectors (Angelopoulos, 2008; McFadden et al., 2008). These data are used to characterize the plasma flows within the magnetotail. The boom-mounted FGM (Auster et al., 2008) data will be used to identify magnetic field line dipolarizations.

Magnetometer and Energetic Particle data from six different GOES spacecraft (GOES 10–15). Details on the GOES 10–12 fluxgate magnetometer data are available at Singer et al. (1996) and the Energetic Particles Sensor data from the Solar Environment Monitor (SEM) are found in Onsager et al. (1996). From the GOES 13–15 spacecraft we also use the fluxgate magnetometer data and particle data from the Magnetospheric Electron Detector (MAGED) within the 30–600 keV energy range (Hanser, 2011; Jaynes et al., 2013).

3. Procedure

We examined by eye THEMIS ASI data for seven stations for 11 years from 2006 to 2016 for examples of auroral omegas. The stations we employed consisted of ones at latitudes that would be associated with auroral omega bands. The list of ASC include ATHA, FSIM, FSMI, GILL, KUUJ, SNKQ, and WHIT and their locations in both geographic and magnetic coordinate are given in Table 1. The procedure for identifying an omega band was the similar to that used in Partamies et al. (2017). Characteristics needed for auroral omega selection were (a) each auroral omega is required to appear in more than one image for a period longer than 2 min, (b) each omega has to resemble the Greek letter Ω over that time range, (c) each auroral omega must propagate east, (d) each auroral omega needs to appear taller than wider for part of its lifetime, and (e) every omega is required to fully fit within the ASC field of view for part of its lifetime for reliable detection. The omega must appear taller than wider for part of its lifetime so the wave in the auroral arc looked more like an "Ω." For all omega-like events we defined the start of the observations, which could include the formation time or the time the structure drifted into the field of view, and the end, which could include the end of the lifetime or the time the structure drifted out of the field of view. If the formation of the auroral omega was observed we identified whether the omega formed from a streamer, east-west arc, or if the formation mechanism was unclear.

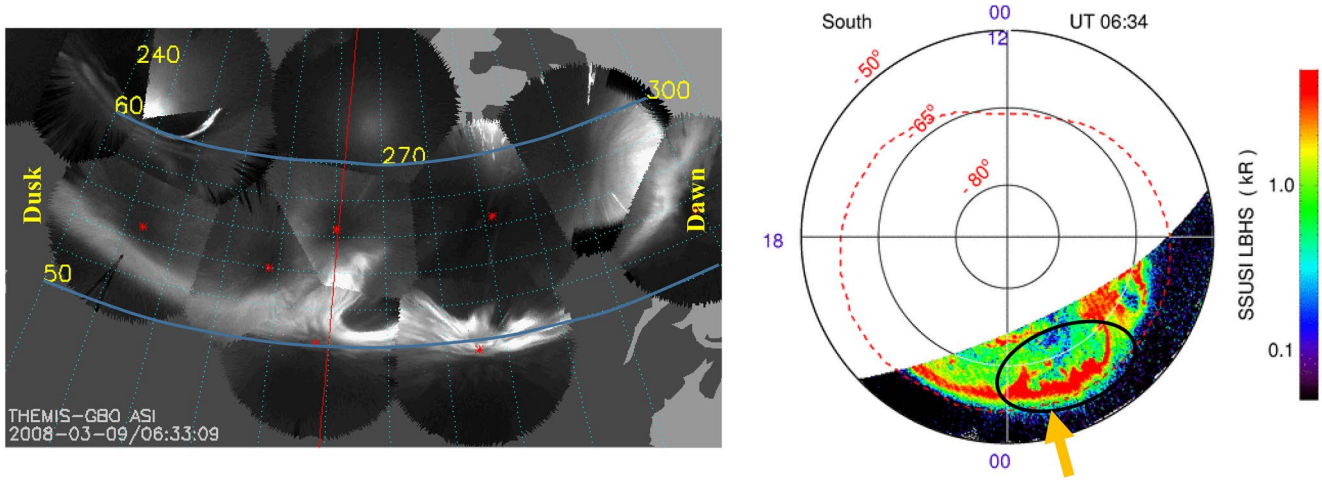

Figure 1. The left side of the figure shows a THEMIS ASI mosaic of a couple of auroral omegas on 9 March 2008 at 0633:09 UT. The coordinate system shown is a geographic coordinate system and local midnight is marked with the red vertical line. The dusk and dawnside of the image have also been labeled. On the right side is a single ultraviolet image of the southern auroral region by DMSP F16 SSUSI. The coordinate system is a magnetic coordinate system with magnetic midnight at the bottom, dawn on the right side, and magnetic noon at the top. The conjugate structures have been circled in black and one clear auroral omega is present between 00 MLT and the orange arrow.

In total we identified 263 auroral omega bands. For each event we determined if the location of the foot points for the THEMIS spacecraft was within the field of view of the ASC or within 1 degree of latitude or longitude. The foot point location was determined using the Tsyganenko 96 magnetic field model (Tsyganenko, 1995). Fifty-one auroral omegas had at least one or more THEMIS spacecraft foot points within or near the ASC field of view. The purpose of this procedure is to help determine the source of the auroral omega bands within the magnetotail.

In addition to the THEMIS ASIs and spacecraft data we examined the DMSP SSUSI auroral image data (Paxton et al., 1992a, 1992b) obtained for the southern hemisphere for examples of hemispherically conjugate auroral omegas. We obtain examples from the 51 auroral omegas with conjugate THEMIS spacecraft data.

4. Observations

In this section we present observations of hemispherically auroral omegas, the formation of auroral omegas from a north-south streamer, and the formation of an auroral omega from an east-west auroral arc.

4.1. Hemispherically Conjugate Auroral Omegas

In Figure 1 we display observations of hemispherically conjugate auroral omegas. The left side of the figure shows a THEMIS ASI mosaic of a couple of auroral omegas on 9 March 2008 at 0633:09 UT. The coordinate system shown is a geographic coordinate system and local midnight is marked with the red vertical line. One clear auroral omega is located at midnight and the other auroral omega is to the right of midnight. On the right side is a single Lyman-Birge-Hopfield short wavelength (140–160 nm) ultraviolet image of a scan of the southern auroral region by DMSP F16 SSUSI with the time of the image given as 0634 UT where the time 0634 UT is the mid-point of the pass through the southern auroral oval. The coordinate system is a magnetic coordinate system with magnetic midnight at the bottom, dawn on the right side, and magnetic noon at the top. The conjugate structures have been circled in black and one clear auroral omega is between 00 MLT and the orange arrow. As far are we are aware this is the first observation of hemispherically conjugate auroral omegas observed in images.

In Figure 2 we present a second example of hemispherically conjugate auroral omegas on 6 April 2010. The format of this figure is the same as Figure 1. The auroral omega in the northern hemisphere occurs is about 5° to the east of local midnight at 0542:48 UT and is circled in black and indicated with the gold arrow. The auroral omega at 0545:00 UT in the DMSP SSUSI image is on the right side and also circled in black as well as marked with the gold arrow. The auroral omega observed by SSUSI is about 15° to the east of magnetic midnight. The shape of the two Ω is surprisingly similar in both hemispheres.

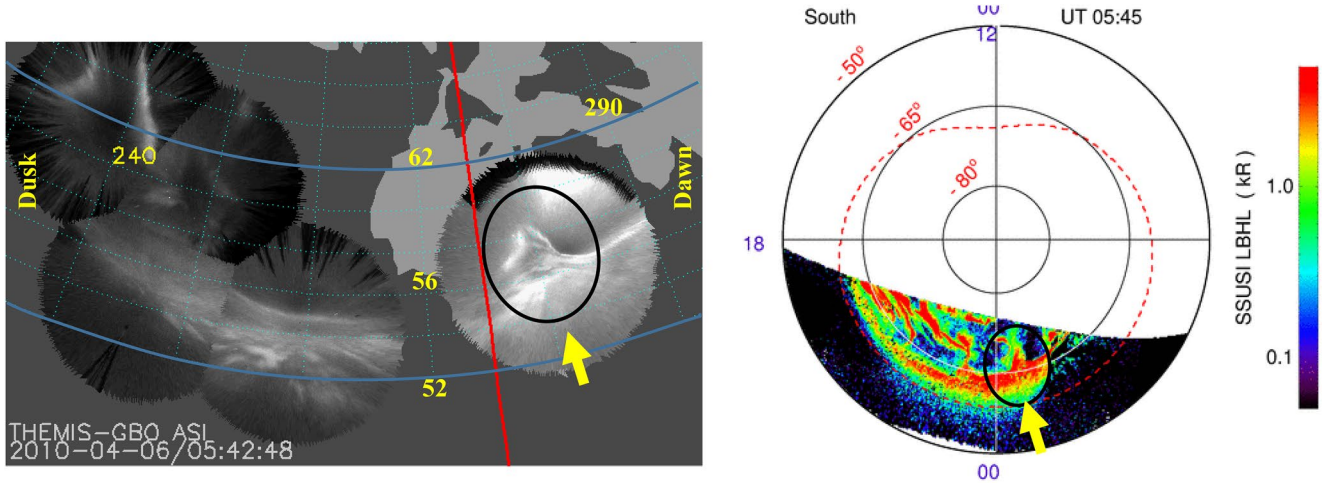

Figure 2. The left side of the figure shows a THEMIS ASI mosaic of an auroral omega on 6 April 2010 at 0542:48 UT and on the right side is a single ultraviolet image of the southern auroral region by DMSP F16 SSUSI. The auroral omega in each image is circled in black and marked with the gold arrow. The format of this image is similar to Figure 1.

We also mapped the edge of the northern hemisphere auroral omegas in both events to the southern hemisphere using the Tsyganenko 01 (T01) magnetic field model (Tsyganenko, 2002a, 2002b), which is appropriate for the active geomagnetic conditions. The magnetic field line trace of the 9 March 2008 auroral shows that the largest auroral omega in the northern hemisphere maps about 5° to the west and several degrees further poleward. The magnetic field line mapping of the 6 April 2010 auroral omega from the northern hemisphere to the southern hemisphere put the feature about 15° to the west, but at the same latitude. We attribute the difference in the location to mapping error and geomagnetic activity, where the AE index is about 750 nT and about 730 nT for each event respectively.

In addition to the hemispherically conjugate auroral observations on 9 March 2008 two other events have been observed on the 21st of August 2014, and seventh of September 2015. In each of these cases the northern auroral omega maps close to but not exactly on top of the southern auroral omega.

4.2. Evolution of Streamer Into Auroral Omega

Figure 3 shows the formation of an auroral omega from a north-south streamer on 1 September 2013. The white haze in the image at about 60° GLat between 270° and 290° GLong north of the auroral omega is light contamination from the town of Sanikiluaq. The vertical red line marks local midnight and indicates the auroral omega forms in the pre-midnight sector less than 1 hr in local time to the west of local midnight. The *E* and *D* within the ASI show the THEMIS spacecraft foot point locations close to the streamer location. THD is about 3° to the west and THE is about 8° to the west and the two spacecraft are about 3 R_E apart within the magnetotail in mainly the X_{GSM} direction at about (−10, 5, 0) R_E. At 0426:30 UT a streamer is present on the far leftside of the SNKQ ASC. By 0427:00 UT the streamer has separated from the poleward edge of the auroral oval and by 0427:30 UT the streamer has become an elongated omega (or auroral torch). At 0429 UT the auroral omega is clear and is slowly propagating eastward. By 0436 UT the auroral omega has nearly collapsed.

Figure 4 displays the THEMIS spacecraft magnetotail observations during this event. The top three panels shows the magnetic field vector, the next three rows show the flow vector, and the bottom panel provides the plasma number density measurements. The vertical green lines show the period over which the auroral omega is present. At about 0430 UT THD measures both earthward flows and dawnward flows above 100 km/s. THE records earthward flows >100 km/s at about 0422 UT, 0425 UT, and 0428 UT as well as strong dawnward flows >150 km/s between 0427 and 0431 UT.

These observations show many of the features we expect for high speed earthward flows as the source of auroral omegas including a north-south streamer that evolves into an auroral omega and high speed earthward flows

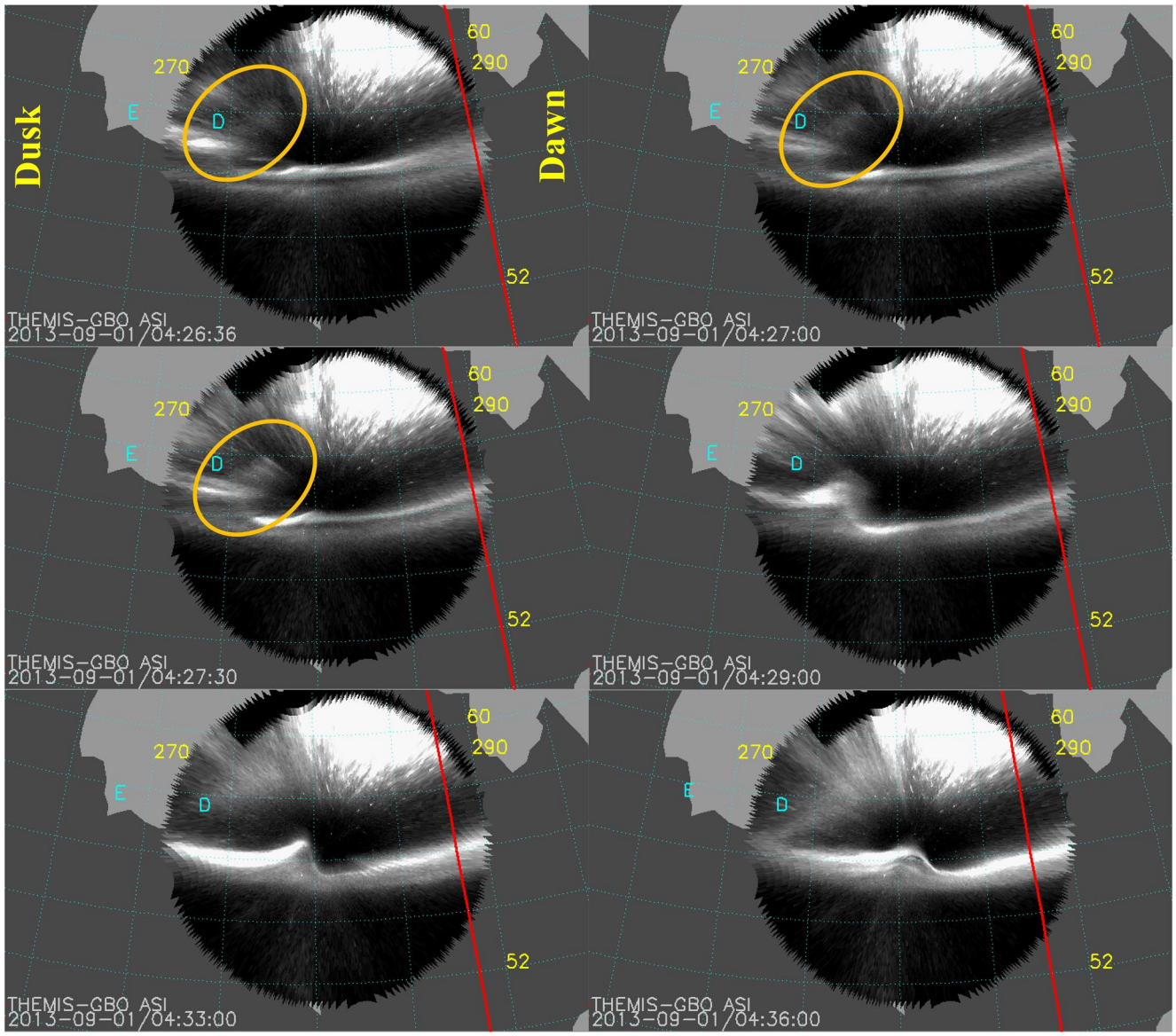

Figure 3. Formation of an auroral omega from a north-south streamer on 1 September 2013. This figure shows several ASIs from the camera at SNKQ. The coordinate system is a geographic coordinate system and the red vertical line marks local midnight. The dusk and dawnside of the image have also been labeled in the first image. The orange oval shows the streamer that evolves into the auroral omega shown at 0429 UT. The E and D indicate the foot points of THEMIS E and D, respectively.

nearly conjugate to the streamer. However, we also see strong dawnward flows that could be associated with a possible shear flow instability.

4.3. Evolution of East-West Are Into Auroral Omega

Figure 5 displays the growth of an auroral omega from an east-west auroral arc observed within the field of view of the FSMI ASC on 13 November 2015. At 1001 UT several east-west arcs are present at the equatorward portion of the auroral oval. There is some auroral activity at the poleward edge of the auroral oval. By 1003 UT an auroral omega within the orange oval has formed from one of the east-west arcs at about 1.5 hr east of local midnight. From 1003 UT to 1010 UT the omega slowly drifts dawnward and after 1010 UT the auroral omega has collapsed. The magnetic foot points of THD and THE are located about 7° to the west of the auroral omega within the field of view of the FSMI ASC. THD and THE are separated by less than 1 R_E in the magnetotail at about (−11, 1, −1) R_E GSM. Figure 6 shows the magnetotail conditions at THD and THE. This figure has the

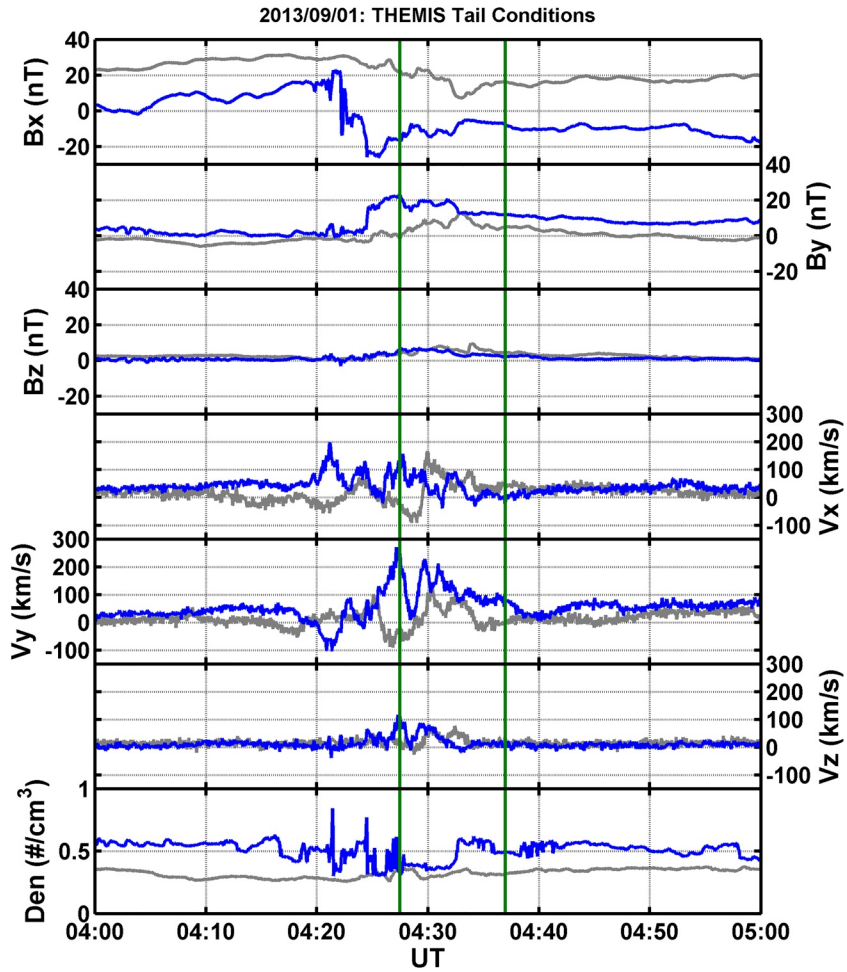

Figure 4. THEMIS D (gray curve) and E (blue curve) magnetotail observations on 1 September 2013. The top three panels are the Bx, By, and Bz magnetic field measurements in GSM coordinates. The next three panels are the flow values and the bottom panel is the plasma number density. The period between the two green vertical lines is when the auroral omega is present in the SNKQ all sky images. High speed earthward flows occur at about 0422 UT and 0427 UT at THE. Earthward flows are observed at THD at about 0430 UT. Strong dawnside flows are present at about 0427 UT to 0430 UT at THE and weaker dawnside flows are observed at THD at about 0430 UT.

same format at Figure 4. At about 0957 UT there is a short period of earthward flow at both THD and THE with a magnitude of about 550 km/s. At the same time V_y flows are about 150 km/s towards the duskside. We also note after the auroral omegas have been observed in the FSMI ASC, one period of high speed earthward flows of about 200 km/s at about 1015 UT occurs and two short periods of dawnside flow of about 200 km/s occurs around 1015 UT.

Just before the formation of the auroral omega the GOES 15 spacecraft records an energetic particle injection. Figure 7 shows an electron energetic particle injection observed in the magnetospheric electron detector (MAGED) data at starting at about 0958 UT. The particle injection is dispersed and begins at about 0958 UT in the 40 keV electrons and later at about 1005 UT in the 475 keV electrons. Magnetic field line mapping indicates that the foot point of GOES 15 is within the field of view of the FSMI ASC.

The observations during this event show conflicting features associated with the different generation mechanisms for auroral omegas. The features we see associated with the theories that high speed earthward flows are the source of auroral omega include high speed earthward flows are shown in Figure 6 and GOES 15 electron (Figure 7) and ion injections (not shown) nearly conjugate to the auroral omega. The features we see associated with the shear flow theory are an omega forming from an east-west arc and dawnside flows, but after the auroral omega observations have occurred.

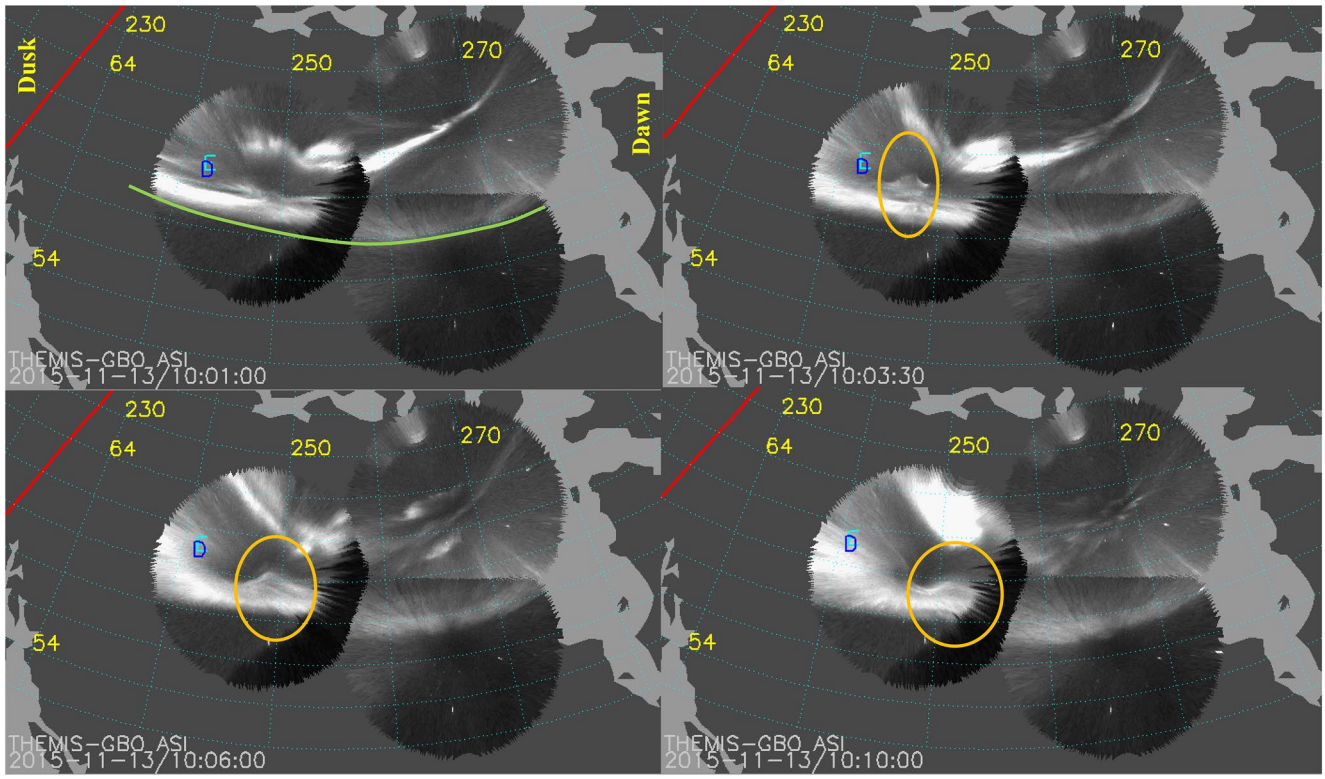

Figure 5. Auroral omega formation on 13 November 2015 at about 1003 UT and ending at about 1010 UT. The format of this figure is similar to Figure 3. This sequence of mosaics consists of all sky images from FSMI, RANK, and GILL. The orange oval shows the location of the auroral omega and the foot points of THD and THE are to the west within the field of view of FSMI. The green arc in the first auroral mosaic indicates the equatorward edge of the auroral oval.

5. Discussion

In the previous section we presented auroral and magnetotail observations associated with auroral omegas that support and conflict with the various theories on auroral omega generation and observations of hemispherically conjugate auroral omegas. We believe that the hemispherically conjugate observations indicate that the magnetotail is the source of auroral omegas. These observations are possibly the first hemispherically conjugate images reported in the literature. It could be argued that the hemispherically conjugate observations on 9 March 2008 may have an ionospheric source because this event occurs near spring equinox when both hemispheres have similar ionospheric characteristics and two other events (6 April 2010 and 7 September 2010) occur within two weeks of equinox conditions. Furthermore, the AMPERE current patterns during the 9 March 2008 event indicate that the auroral omegas are basically between the region 1 downward currents and region 2 upward currents and both locations are within the unlit portion of the ionosphere, but the SuperDARN convection patterns and potential patterns (not shown) are not the same in both hemispheres. The flow patterns show that the auroral omega in the northern hemisphere may be co-located with an ionospheric flow shear in the duskside convection cell, while the observations in the southern hemisphere appear to correspond to eastward ionospheric flows in the dawnside convection cell. Moreover, the hemispherically conjugate omega event on 21st of August 2014, when both hemispheres are most likely dissimilar to one another, does not support the idea that the ionosphere could be the source of auroral omegas.

The observations of the auroral omega forming from the north-south streamer and from the east-west auroral arc shown in the Observation section had ambiguous magnetotail observations. Both had near conjugate observations by the THEMIS spacecraft consistent with both the high speed earthward flows and dawnside shear like flows. In this section we perform a simple statistical analysis of the 51 auroral omegas with conjugate THEMIS spacecraft data. To obtain these statistics we systematically examine the data from all the events and look for features consistent with each theory. For the high speed earthward flow theory we look for an auroral streamer that evolves into an omega, high speed earthward flows >100 km/s at the near conjugate THEMIS spacecraft, B_z magnetic

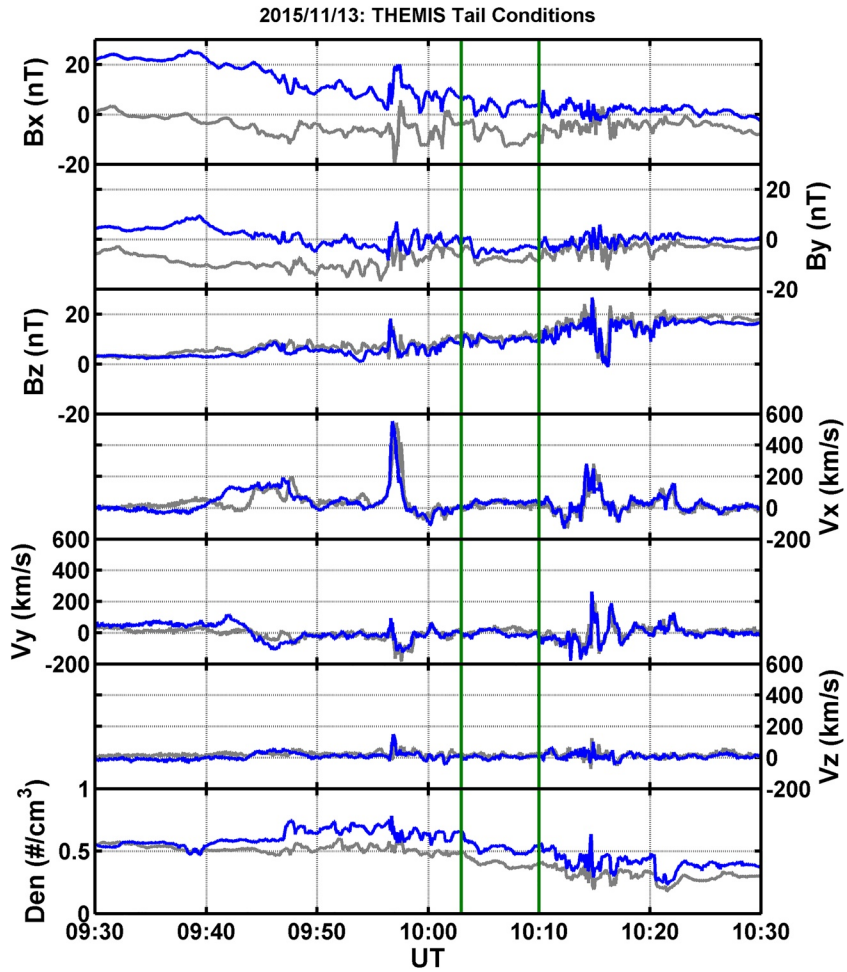

Figure 6. This figure has the same format as Figure 4 and displays the magnetotail conditions at THD and THE. The observations of the auroral omega occur between the two vertical lines.

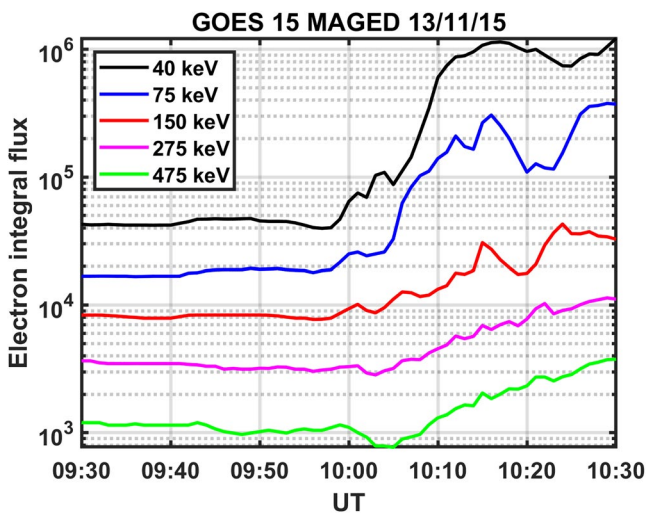

Figure 7. GOES MAGED energetic electron integral flux data for 13 November 2015. Five different energy channels are shown. The electron injection begins at about 0958 UT in the 40 keV electrons.

field dipolarizations, and energetic particle injections at the GOES spacecraft that are associated high speed earthward flows. The choice of 100 km/s is arbitrary but consistent with prior studies of high speed flows (Juusola et al., 2011; Sigsbee et al., 2002; Weygand et al., 2015) and this value is meant to be greater than nominal magnetotail convection speeds (Nishida et al., 1998). For the shear flow theory we search the data for an east-west arc that appears to evolve into an omega and a flow shear in the post-midnight sector or at least strong dawnward flows. Since it is unlikely we will find a flow shear unless the spacecraft quickly traverses the post-midnight sector in the radial direction, we concentrated on searching for strong dawnward flows.

Requirement for a value for a flow "strong" enough to produce a KHI depends on local magnetic field orientation with respect to maximum flow shear and plasma density gradient across the flow shear. Magnetic field component along *k*-vector, magnetic field curvature with line tying to the ionosphere, and plasma compressibility can all stabilize KHI. However, often a range of angles can exist along which the KH *k*-vector has a positive growth rate (Nykyri et al., 2021). Assuming the KHI onset condition in the magnetotail is satisfied along Y_{GSM} direction, the phase speed along this direction can be estimated from:

Table 2
Estimated Dawnward Flow Values to Obtain KHI From THEMIS and Auroral Omega Measurements

Event (yyyymmdd)	n_1 (#/cm^3)	v_1 (km/s)	n_2 (#/cm^3)	V_{KHI} (km/s)	v_2 (km/s)
20080210	0.60	−3	0.50	−22.5	−45.8 (−100)
20130817	0.60	−3	0.27	−42.1	−128 (−50)
average	0.6	−3	0.38	−32.3	−86.9

$$\boldsymbol{V}_{KHI} = \frac{(n_1\boldsymbol{v}_1 + n_2\boldsymbol{v}_2)}{(n_1 + n_2)} \quad (1)$$

where V_{KHI} is used as the speed of the auroral omega, n_1 is the density of the inner plasma, v_1 is the velocity of the inner plasma along Y_{GSM} direction, n_2 is the density of the outer plasma, and v_2 is the velocity of the plasma flowing past the inner plasma along Y_{GSM} direction. Magnetic field line mapping of the auroral omegas indicates that the region associated with this possible instability is most likely at about 6–8 R_E down the tail between about 23 and 06 MLT (Weygand et al., 2015; Partamies et al., 2017). Based on the mapping of the auroral omegas let us assume that the inner boundary is at about geosynchronous orbit and is moving with the corotation speed then the speed v_1 is about 3 km/s. There are approximately 2 auroral omega events of the 51 with near conjugate spacecraft data such that the distribution and motion of the near conjugate THEMIS spacecraft could be used to roughly estimate n_1, n_2, and V_{KHI} and obtain a threshold value for v_2 that would produce the KHI/auroral omega.

To obtain the values for V_{KHI} we mapped five points for each auroral omega of the 2 events from the ionosphere to the equatorial plane for three different times using the T01 magnetic field line model (Tsyganenko, 2002a, 2002b). These mapped locations and times were used to obtain the azimuthal speeds. See Table 2, fifth column. The dawnward speeds we obtain for the auroral omega in the magnetotail are 22.5 and 42.1 km/s. These values for the tail component of the auroral omegas are similar to the 30 km/s and 70 km/s obtained for the auroral omegas in Weygand et al. (2015) and Liu et al. (2018), respectively.

To find the flow shear values v_2 from Equation 1 that would potentially produce KHI auroral omegas we require the density n_1 of the inner plasma closest to the earth and the density n_2 of the outer plasma farther from the earth. These values were estimated by finding auroral omega events that form from east-west arcs and have near conjugate THEMIS spacecraft moving radially across the region where the auroral omega maps. We did not have any events where THEMIS spacecraft were distributed radially across the auroral omega, however, we have two events where the THEMIS spacecraft are initially between 11 to 13 Re, then move radially inward to about 6.6 Re. In all two cases the density n_2 is measured at about the time of the auroral omega while the density n_1 is obtained hours later. In all these cases we have assumed that the density in the inner magnetosphere has not changed. This assumption is highly questionable. In the best case on 17 August 2013 the density n_1 is measured 2 hr later. The measured values for n_1, n_2, and the calculated shear flow value v_2 from Equation 1 (and the THEMIS measured value) are given in Table 2. The lowest value we obtain from this exercise is approximately 45 km/s dawnward, which is not much more than the convection speed. This value seems unreasonably low and would suggest there are potentially KHIs occurring quite frequently, but we will use −50 km/s as the cutoff value and lowest estimate for our statistical analysis in the next section.

5.1. Statistics

For each of the 51 auroral omega events with near conjugate magnetotail spacecraft data and good auroral images we searched both the spacecraft data and image data to features consistent with the high speed earthward flow mechanism and the KHI source. We only consider features from 15 min before the auroral omega to 5 min after the omega. Furthermore, we required the B_x component to be ≤5 nT to provide confidence that the THEMS spacecraft were within the plasma sheet. Twenty-two of the ASIs showed auroral omegas evolving from north-south streamers with an average duration of 11.5 min and 13 had auroral omegas forming from east-west arcs with an average duration of 6.9 min. We note that of 13 of the omegas from east-west arcs 5 had a streamer located to the west of the omega. In summary, nearly twice as many auroral omegas were observed evolving from north-south streamers then from east-west arcs. This ratio is quite different from Weygand et al. (2015) where 10 of the omega bands appeared to develop out of east-west arcs and 5 Ω evolved from streamers. The biggest difference between the Weygand et al. (2015) study and this one is that Weygand et al. (2015) only examined one period with many auroral omegas where the tail conditions may have been similar for the entire period and this study has reviewed over 51 separate auroral omega periods.

Of the 51 auroral omegas 19 showed evidence of magnetic field dipolarizations and/or energetic particle injections. To be considered a particle injection in this study the injection could occur in the electrons, ions, or both and the injection had to be present in at least two energy channels. We did not differentiate between dispersionless or dispersed injections. However, nearly all events were dispersionless. In the THEMIS FGM data 34 of 51 events had features of dipolarizations in the B_z component of the magnetic field and seven of the 51 had high speed earthward flows greater than 100 km/s present in the ESA data. In total 41 (80%) of 51 events with spacecraft data had at least one feature or a combination of features consistent with high speed earthward flows occurring nearly conjugate to the auroral omega and within 15 min before the auroral omega or 5 min after. Of these, in 19 of these 41 auroral omegas, the omega developed from a streamer.

The number of events with dawnward flows ≥50 km/s was considerably less. Five (~10%) of 51 events had significant dawnward flow within the allotted time window and 4 of these events were also associated with observations of high speed earthward flows, dipolarizations in the magnetic field, or energetic particle injection observed at THEMIS and/or GOES. Furthermore, only two of the 5 events also showed auroral omegas forming from east-west arcs and one of the two showed features of high speed earthward flows, dipolarizations in the magnetic field, or energetic particle injections observed at THEMIS and/or GOES. We would also like to note that there were 6 events with duskward flows ≥50 km/s and five of these events were also associated with observations of high speed earthward flows, dipolarizations in the magnetic field, or energetic particle injections observed at THEMIS and/or GOES. Only one of these events formed from an east-west auroral arc. This mixture of features does not clearly support the idea that auroral omegas are produced solely by KHIs at the boundary between the inner magnetosphere and the earthward edge of the plasma sheet (Janhunen & Huuskonen, 1993; Rostoker and Samson, 1984). Additional detailed auroral omega statistics can be found in the supplementary material.

Our statistics suggest that high speed earthward flows (Roux et al., 1991; Henderson, 2009, 2012) are the most common mechanism for producing auroral omegas. There are numerous observations of auroral omegas forming from streamers (Henderson, 2009, 2012), but few studies with magnetotail observations. Those studies with near conjugate tail data do show enhanced Alfvénic Poynting flux and transient bursts of electron differential energy flux parallel to the magnetic field with dispersed energy signatures when satellite foot points were located in the vicinity of the omega bands (Wild et al., 2011) and high speed earthward flows. Our observations and those of prior studies do not entirely exclude the theory of Yamamoto (2011), that the hybrid Kelvin-Helmholtz/Rayleigh-Taylor (KH/RT) instability as the source of auroral omegas. In that mechanism, earthward directed bursty bulk flows within the magnetotail result from the KH/RT instability, leading to the formation of north-south streamer auroras, and the auroral omegas are the end result of streamers. The mixture of features associated with high speed earthward flows as well as significant dawnward flows support this mechanism, but Yamamoto (2011) shows the development of omega like features from streamers, which is not what was observed for most of our 5 events with significant dawnward flow. Only 2 (4%) of the auroral omegas developed from north-south streamers and had features of both earthward flows and significant dawnward flows. Furthermore, Yamamoto (2011) does not address how auroral omegas can form from east-west auroral arcs.

5.2. MHD Results

In addition to the auroral images and spacecraft data, we simulated the magnetosphere during the auroral omegas observed on 9 March 2008 using a global MHD model (El-Alaoui et al., 2001; Raeder et al., 1995) to investigate in detail a few auroral omega events. Spacecraft observations only cover a small portion of the magnetotail and do not capture all the magnetotail features relevant to omega formation. The purpose of the MHD simulation is to ascertain whether high speed earthward flows and/or azimuthal flow shears are present in the magnetotail for different auroral observations of omega formation. For this task we simulated the magnetotail during observations of auroral omegas on 9 March 2008 that formed from an auroral streamer and from an east-west arc. The observations have been discussed in detail in Weygand et al. (2015). The auroral omegas are shown in Figure 8, which is a series of THEMIS ASI mosaics. These mosaics have nearly the same format as Figure 3. The orange oval at time 0618 UT shows the several north-south streamers together, which began at about 0606 UT, and by 0627:09 UT the streamers have broken away from the northern edge of the auroral oval to become an auroral omega and a torch. The torch and the auroral omega map between 6 and 20 R_E down tail and between about 0 and 2 R_E Y_{GSM}. By 0632:21 UT the structures have become two auroral omegas and these omegas are no longer visible by about 0640 UT. The yellow circle at 0622:39 UT shows an omega forming from an east-west arc and by 0627:09 UT an

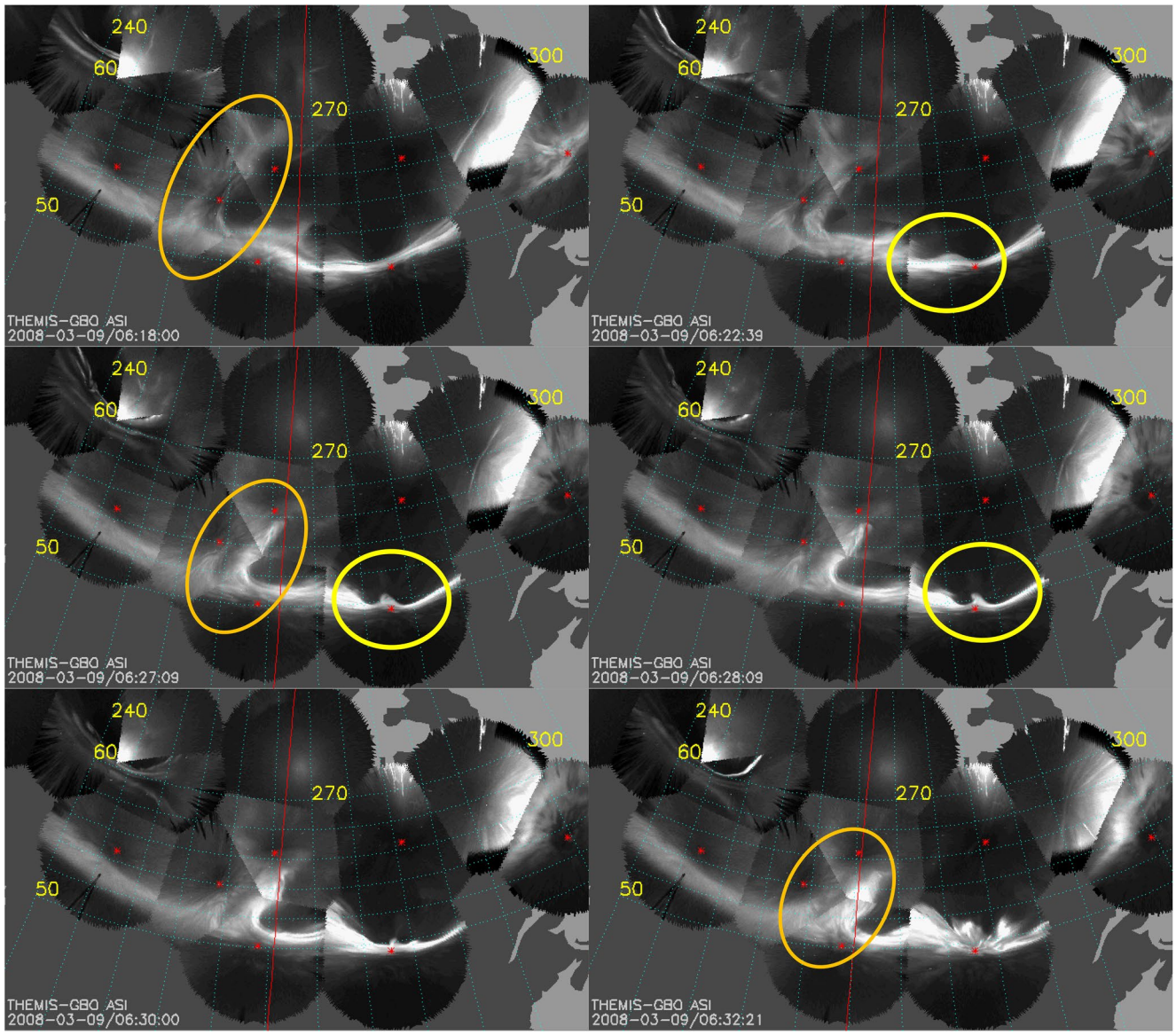

Figure 8. Series of THEMIS ASI mosaics from 9 March 2008. These mosaics have the same format as Figure 3. The orange circle at time 0618 UT shows the several north-south streamers and at 0627:09 UT the streamers have become an auroral omega and a torch. By 0632:21 UT the features have become two auroral omegas. The yellow circle at 0622:39 UT shows an omega forming from an east-west arc and by 0627:09 UT an auroral omega is present. Then by 0630:00 UT the omega has nearly collapsed back into an east-west arc.

auroral omega is present and propagates dawnward for several minutes. Then by 0630:00 UT the omega has nearly collapsed back into an east-west arc. The multiple high speed earthward flows are present in the magnetotail, but not at the same time as the streamers. See Figure 8 of Weygand et al. (2015). THB-THE observations were available during this period, but spacecraft appeared to be about 5 R_E further to the dusk. GOES 12 also appears to show a dipolarization in the northward component of the magnetic field at about 0628 UT, but this spacecraft is 2 R_E off towards the dawnside. Modeling this omega event provides important context for the tail observations.

The state of the magnetotail during the MHD simulation of the magnetosphere on 9 March 2008 has been discussed in Peroomian et al. (2014). The MHD simulation results between 0623 UT and 0647 UT suggest that potentially both high speed flows and flow shears are responsible for the auroral omega bands observed in the ASIs between 0606 UT and 0631 UT. Figure 9 shows two different times from the MHD simulations of that period with high speed earthward flows and flow shears. In Figure 9 the sun is to the right, the duskside of the magnetosphere is at the top of the panel, and the dawnside is at the bottom. The left side of Figure 9 shows a

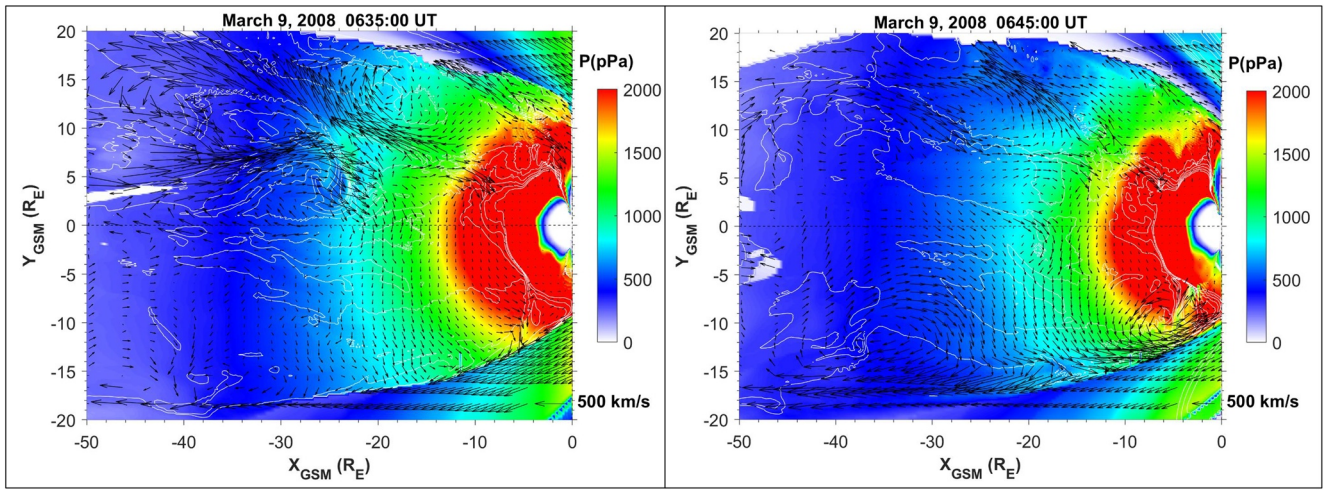

Figure 9. Results from global MHD simulation for 2008. The vectors indicate the flow in the X and YGSM and the key is in the lower right corner. The color indicates the plasma pressure and the color bar is on the right side of the figure. The left panel shows high speed earthward flows coming in at about (−22, 5) R_E GSM and the shear flow in the post-dawn sector. The right panel shows high speed earthward flows coming in at about (−20, 7) R_E GSM and the shear flow in the post-dawn sector.

minimum magnetic field surface in the magnetotail at 0635 UT with the high speed earthward flows on the order of 120–400 km/s at between −30 and −10 R_E X_{GSM} and about 5 R_E Y_{GSM} (at about 23 MLT). These flows begin at about 0628 UT and last until 0637 UT. From 0631 UT to 0636 UT some of these earthward flows divert dawnward with speeds between 60 and 120 km/s at about 10–15 R_E down tail. At about −10, 5 R_E GSM pressure at the inner magnetosphere begins to build up.

The right side of Figure 9 shows a second period of high speed earthward flows with a dawnside flow shear. The high speed flows begin at about 0643 UT and last until about 0648 UT and penetrate into about −12 R_E X_{GSM} from −40 R_E XGSM at about 7 R_E Y_{GSM} with speed between 210 and 650 km/s. Like the last period shown, a large flow shear appears in the dawnside of the tail at about −12 R_E GSM between about 22 and 4 MLT. This shear begins at about 0644 UT and ends at 06248 UT. At about −11, 5 R_E GSM, pressure at the inner magnetosphere begins to build up. In total three high speed earthward flows are observed between 0623 UT and 0648 UT in the pre-midnight sector and four periods of shear flows in the post-midnight sector. All three of the earthward flows lead to dawnside flows shears. Only two events have been shown in Figure 9.

The timing of the high speed earthward flows and shear flow in the MHD simulation does not match the auroral observations, but this is not uncommon for MHD simulations. What is interesting is the order, the location, and durations of the observations in the MHD simulation for both periods shown in Figure 9. For the first event shown in Figure 9 the simulation high speed earthward flows begin at about 0623 UT and last 3 min in a similar location ((−20, 5) R_E GSM) as the magnetic field line mapped observations of the streamers and the auroral omegas (∼15, 1) R_E GSM, which lasted in total about 34 min. See Figure 7 in Weygand et al. (2015). Similarly, the MHD shear flow in the simulations begins toward the end of the high speed earthward flow and lasts about 4 min in the postmidnight sector, whereas the observed auroral omega from the east-west arc starts about 14 min after the streamers and lasts for about 8 min at 0.5 MLT. Similar observations are present for the second event shown in Figure 9. We conclude that the order of the earthward flows and dawnward flows in the MHD simulation for the 9 March 2008 periods is consistent with the formation of the auroral omegas from the streamers and then the formation of the auroral omega from the east-west arc recorded in the observations. However, in each of the periods from the simulations the duration of the high speed earth flows and the dawnside flow shears is significantly less than the observed duration of the auroral omegas from north-south streamers (11.5 min) and from east-west arcs (6.9 min).

Another way to evaluate the plausibility of KH instability that could be produced by the azimuthal velocity shear in the magnetosphere and could be responsible for auroral omega is to use the concept of magnetic flux, $\Phi = BA$, conservation such that $\Phi_I = \Phi_M$. Using the magnetic field strength in ionosphere (B_i) and magnetosphere (B_m), respectively, and the area of the auroral omega (A_i), the required KH instability vortex size in the

Table 3
This Table Provides Estimate of the Area of the Auroral Omegas in the Ionosphere, the Magnetic Field in the Vertical Direction at the Auroral Omega in the Ionosphere, Magnetic Field in the Z_{GSM} Direction in the Magnetotail, the Area of the Auroral Omega According to Conservation of Flux, and the Derived Velocity Shear Thickness Given in Equation 2

Event yyyymmdd UT	A_i (measured) (km^2)	B_i (nT)	B_m (nT)	$A_m = A_i (B_i/B_m)$	Velocity shear thickness (km)
20080210 1223 UT	11,812	53,091	3.4	1.84×10^8	3.6×10^3
20130817 0447 UT	9,812.1	53,096	4.1	1.27×10^8	3.0×10^3

equatorial nightside magnetosphere is expected to be $A_m = \frac{B_i A_i}{B_m}$. Because the fastest growing KH instability wave length, λ=(2–4)$\pi\Delta$, where Δ is the velocity shear layer thickness, and the vortex diameter is typically 1/3 of the wave length, the area of the vortex can be estimated as $A_m = \pi\lambda^2/9$. This will yield a velocity shear layer thickness of

$$\frac{(0.25 \ to \ 0.5)\sqrt{\frac{9B_iA_i}{B_m}}}{\pi\left\{\frac{3}{2}\right\}} \quad (2)$$

Using Figure 9 we get an estimated velocity shear thickness of about 6–8 R_E (38,269 to 51,025 km) just to the dawnside of the Y GSM axis. With the two auroral omega events examined in Table 2 we can get two estimates of the velocity shear thickness layer. The area of auroral omegas in the ionosphere can be measured with the auroral images. The magnetic field at the auroral omega in the ionosphere and within the magnetotail tail can be estimated with the Tsyganenko 96 model. Table 3 provides the estimated values including the values derived for the velocity shear thickness layer, using a multiplying factor of 0.5 on Equation 2 to produces the largest shear thickness. Table 3 clearly shows that the calculated velocity shear thickness is approximately a factor of 10 smaller than the velocity shear thickness layer obtained from the MHD model. These results suggest that auroral omegas are most likely not produced by KH instabilities. Even if we estimate A_m by magnetic field line tracing the auroral omegas into the magnetotail and inserting this A_m value in Equation 2, the velocity shear thickness values are still much smaller than the estimates from the MHD model.

We have presented evidence from a variety of ground and space based instrumentation and a MHD model simulation showing that high speed flows occurred in the near magnetotail for most of our auroral omega observations. Our interpretation of the auroral omegas forming from north-south streamers remains the same as the description and Figure 14 from Weygand et al. (2015). The observations and simulation shown in this study build upon the prior description and suggest that the auroral omegas from east-west arcs may be the result of plasma flow diverting dawnward and producing an instability (possibly a KHI) that creates omega like formations within the east-west arcs, but these omegas are short lived. This simplistic hypothesis indicates that the auroral omegas produced from the diverted flows would most likely have a distribution in MLT that peaks further dawnward then those auroral omegas produced directly from high speed earthward flows. Figure 10 shows that two different distributions of auroral omegas appear to be present. With the limited number of auroral omegas available we have plotted the MLT distribution of auroral omegas observed to form directly from auroral north-south streamers (black bars), which peaks at 1 MLT, and auroral omegas from east-west auroral arcs (blue bars), which peaks at 3 MLT. The medians, means, and error of the means of the two distributions are 1 MLT, 1 MLT, and ±0.3; and 2.3, 1.8 MLT, and ±0.4 MLT, respectively. The mean and the error of the mean demonstrate that the two distributions are statistically different, but not by much.

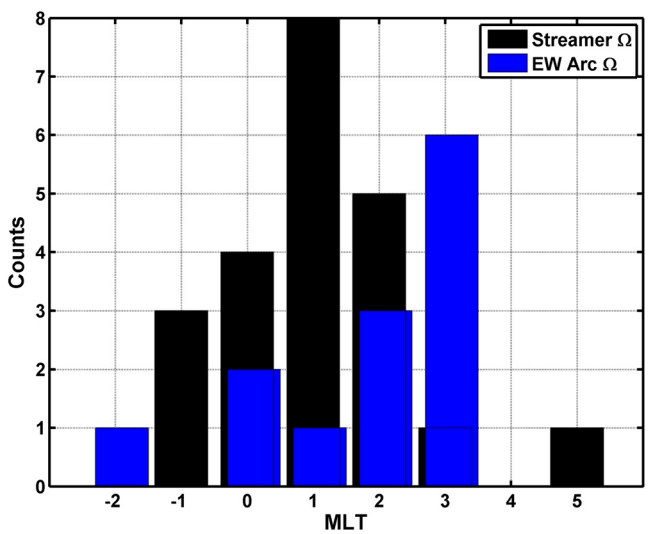

Figure 10. Histograms of two different auroral omegas. The black bars are of auroral omegas observed to form directly from auroral north-south streamers and the blue bars are the distribution of auroral omegas from east-west auroral arcs.

An interesting difference between the MHD result of the Weygand et al. (2015) and the MHD results of this study is the lack of undulations in the pressure surfaces at the inner magnetosphere. Figure 13 of Weygand et al. (2015) showed undulations in the pressure surfaces at the inner part of the magnetosphere. These undulations propagated dawnward at about the same speed as the auroral omegas and resembled the magnetic field line mapped auroral omegas. However, the simulation in Weygand et al. (2015) was not of an auroral omega event. What is unclear is whether these undulations are related to auroral omegas or if the auroral omegas are produced by the significant dawnward flows as observed in this studies MHD simulation, reported here, of an actual period with auroral omegas. What is still missing is conjugate spacecraft observations within and/or surrounding the auroral omegas formed from east-west arcs.

6. Summary and Conclusion

We have identified 51 of the 263 auroral omegas in the THEMIS ASI data that have conjugate or near conjugate THEMIS and GOES spacecraft data. We have examined the magnetotail data for evidence of high speed earthward flows, magnetic field dipolarizations, energetic particle injections, and significant dawnward flows to try and determine the generation mechanism for these auroral omegas. Our significant findings are:

1. We have shown the first evidence of hemispherically conjugate auroral omegas and have four examples of conjugate omegas. These observations indicate that the magnetotail is the source of auroral omegas
2. There is evidence in about 80% of these 51 events that high speed earthward flows, energetic particle injections, and dipolarizations have occurred prior to or at about the same time as the auroral omega observation
3. Twenty–two of 51 events developed from north-south streamers and 13 of 51 evolved from east-west arcs. The means of formation for the rest could not be determined
4. Of the 22 auroral omegas from streamers, 4 had earthward high speed flows and 19 events had dipolarizations and energetic particle injections. Two events also had significant dawnward flos
5. Of the 13 auroral omegas from east-west arcs, only 1 had earthward high speed flows and 11 events had dipolarizations and energetic particle injections. Two events had significant dawnward flows and one event has duskward flows
6. For the 16 auroral omegas where the formation was ambiguous, only two had earthward high speed flows and 11 events had dipolarizations and energetic particle injections. One event had significant dawnward flows and one event had duskward flows
7. Only 5 events show evidence of significant dawnward flows and only two developed from east-west arcs. Four of the 5 auroral omegas also show evidence of earthward high speed flows
8. MHD models also suggest that auroral omegas develop from high speed earthward flows and potentially from dawnward flows resulting from the diversion of earthward flows. However, it is still unclear whether auroral omegas develop from shears in the post-midnight sector. Estimates of the velocity shear thickness from the MHD model do not match theoretical estimates

For this study we examined 10 years of ASI data from 7 different ASCs and we have shown a strong correlation between high speed earthward flows and auroral omegas especially those formed from north-south streamers. A question that is still unanswered is why do not all north-south streamers produce auroral omegas. There is still a large archive of data to help better understand the formation of auroral omegas from east-west arcs. It is still not entirely clear whether these auroral omegas from east-west arcs are the result of some instability or the result of corrugations of pressure surfaces that resembled the magnetotail mapped omega as discussed in Weygand et al. (2015). Clearly more work is required to understand this subset of auroral omegas.

Acknowledgments
We acknowledge NASA awards 80NSSC18K0719 and 80NSSC18K1220, NASA THEMIS contract NAS5-02099, NASA HPDE contract 80GSFC17C0018 at UCLA. KN acknowledges the support from NASA Grants #NNX16AF89G and #NNX17AI50G. We thank the members of the THEMIS team for providing the THEMIS ASIs at http://themis-data.igpp.ucla.edu/thg/l1/asi/ and THEMIS spacecraft data at https://cdaweb.gsfc.nasa.gov/pub/data/themis/. We also thank DMSP SSUSI team for providing the conjugate SSUSSI auroral images at https://ssusi.jhuapl.edu/gal_Aur. Finally we also thank NOAA for making the GOES magnetometer and energetic particle data available at https://satdat.ngdc.noaa.gov/sem/goes/data/. We would also like to thank Dr. R.J. Strangeway, Dr. T. Nishimura, Dr. M.G. Kivelson, Dr. Krishan Khurana, and Dr. R.J. Walker for their invaluable input.

References

Akasofu, S.-I., & Kimball, D. S. (1964). The dynamics of the aurora, 1. Instabilities of the aurora. *Journal of Atmospheric and Terrestrial Physics*, *26*, 205–211. https://doi.org/10.1016/0021-9169(64)90147-3

Amm, O. (1996). Improved electrodynamic modeling of an omega band and analysis of its current system. *Journal of Geophysical Research*, *101*, 2677–2683. https://doi.org/10.1029/95ja03155

Amm, O., Aksnes, A., Stadsnes, J., Østgaard, N., Vondrak, R. R., Germany, G. A., et al. (2005). Mesoscale ionospheric electrodynamics of omega bands determined from ground-based electromagnetic and satellite optical observations. *Annals of Geophysics*, *23*, 325–342. https://doi.org/10.5194/angeo-23-325-2005

André, D., & Baumjohann, W. W. (1982). Joint two-dimensional observations of ground magnetic and ionospheric electric fields associated with auroral currents, 5. Current system associated with eastward drifting omega bands. *Journal of Geophysics*, *50*, 194.

Angelopoulos, V. (2008). The THEMIS mission. *Space Science Reviews*, *141*, 5–34. https://doi.org/10.1007/s11214-008-9336-1

Auster, H. U., Glassmeier, K. H., Magnes, W., Aydogar, O., Baumjohann, W., Constantinescu, D., et al. (2008). The THEMS, fluxgate magnetometer. *Space Science Reviews*, *141*, 235–264. https://doi.org/10.1007/s11214-008-9365-9

Donovan, E., Mende, S., Jackel, B., Frey, H., Syrjasuo, M., Voronkov, I., et al. (2006). The THEMIS all-sky imaging array–systems design and initial results from the proto type imager. *Journal of Atmospheric and Solar-Terrestrial Physics*, *68*, 1472–1487. https://doi.org/10.1016/j.jastp.2005.03.027

El-Alaoui, M. (2001). Current disruption during November 24, 1996 substorm. *Journal of Geophysical Research*, *106*, 6229–6245. https://doi.org/10.1029/1999JA000260

Gustafsson, G., Baumjohann, W., & Iversen, I. I. (1981). Multi-method observations and modeling of the three-dimensional currents associates with a very strong Ps 6 event. *Journal of Geophysics*, *49*, 138.

Hanser, F. A. (2011). EPS/HEPAD calibration and data handbook, Tech. Rep. GOESN-ENG-048D, assurance Technology corporation, Carlisle, mass. Retrieved from http://www.ngdc.noaa.gov/stp/satellite/goes/documentation.html

Henderson, M. G. (2009). Observational evidence for an inside-out substorm onset scenario. *Annals of Geophysics*, *27*, 2129–2140. https://doi.org/10.5194/angeo-27-2129-2009

Henderson, M. G. (2012). Auroral substorms, poleward boundary activations, auroral streamers, omega bands, and onset precursor activity. *Auroral phenomenology and magnetospheric processes: Earth and other planets*, 39–54. https://doi.org/10.1029/2011GM001165

Henderson, M. G., Kepko, L., Spence, H. E., Conners, M., Sigwarth, J. B., Frank, L. A., et al. (2002). In R. M. Winglee (Ed.), *The evolution of north-south aligned auroral forms into auroral torch structures: The generation of omega bands and Ps6 pulsations via flow bursts, Sixth international conference on substorms*. University of Washington.

Henderson, M. G., Reeves, G. D., & Murphree, J. S. (1998). Are north-south aligned auroral structures an ionospheric manifestation of bursty bulk flows? *Geophysical Research Letters*, *25*, 3737–3740. https://doi.org/10.1029/98gl02692

Janhunen, P., & Huuskonen, A. (1993). A numerical ionosphere magnetosphere coupling model with variable conductivities. *Journal of Geophysical Research*, *98*, 9519–9530. https://doi.org/10.1029/92ja02973

Jaynes, A. N., Lessard, M. R., Rodriguez, J. V., Donovan, E., Loto'aniu, T. M., & Rychert, K. (2013). Pulsating auroral electron flux modulations in the equatorial magnetosphere. *Journal of Geophysical Research: Space Physics*, *118*, 4884–4894. https://doi.org/10.1002/jgra.50434

Juusola, L., Østgaard, N., Tanskanen, E., Partamies, N., & Snekvik, K. (2011). Earthward plasma sheet flows during substorm phases. *Journal of Geophysical Research: Space Physics*, *116*(A10). https://doi.org/10.1029/2011ja016852

Kawasaki, K., & Rostoker, G. (1979). Perturbation magnetic fields and current systems associated with eastward drifting auroral structures. *Journal of Geophysical Research*, *84*, 1464. https://doi.org/10.1029/ja084ia04p01464

Keskinen, M. J., Mitchell, H. G., Fedder, J. A., Satyanarayana, P., Zalesak, S. T., & Huba, J. D. (1988). Nonlinear evolution of the Kelvin-Helmholtz instability in the high-latitude ionosphere. *Journal of Geophysical Research*, *93*(A1), 137–152. https://doi.org/10.1029/ja093ia01p00137

Liu, J., Lyons, L. R., Archer, W. E., Lacourt, B. G., Nishimura, Y., Gabrielse, C., et al. (2018). Flow shears at the poleward boundary of omega bands observed during conjunctions of Swarm and THEMIS ASI. *Geophysical Research Letters*, *45*(3), 1218–1227. https://doi.org/10.1002/2017gl076485

Lühr, H., & Schlegel, K. (1994). Combined measurements of EISCAT and the EISCAT magnetometer cross to study bands. *Journal of Geophysical Research*, *99*, 8951.

McFadden, J. P., Carlson, C. W., Larson, D., Ludham, M., Abiad, R., Elliott, B., et al. (2008). The THEMIS, ESA plasma instrument and In-flight Calibration. *Space Science Reviews*, *141*, 277–302. https://doi.org/10.1007/s11214-008-9440-2

Mende, S. B., Harris, S. E., Frey, H. U., Angelopoulos, V., Russell, C. T., Donovan, E., et al. (2008). The THEMIS array of ground-based observatories for the study of auroral substorms. *Space Science Reviews*, *141*, 357–387. https://doi.org/10.1007/s11214-008-9380-x

Mravlag, E., Scourfield, M. W. J., Walker, A. D. M., Sutcliffe, P. R., & Nielsen, E. (1991). Simultaneous observations of omega band related phenomena in both hemispheres. *Journal of Atmospheric and Terrestrial Physics*, *53*, 309–317. https://doi.org/10.1016/0021-9169(91)90114-m

Nishida, A., Mukai, T., Yamamoto, T., Kokubun, S., & Maezawa, K. (1998). A unified model of the magnetotail convection in geomagnetically quiet and active times. *Journal of Geophysical Research*, *103*(A3), 4409–4418. https://doi.org/10.1029/97ja01617

Nishimura, Y., Lyons, L. R., Angelopoulos, V., Kikuchi, T., Zou, S., & Mende, S. B. (2011). Relations between multiple auroral streamers, pre-onset thin arc formation, and substorm auroral onset. *Journal of Geophysical Research*, *116*, A09214. https://doi.org/10.1029/2011JA016768

Nykyri, K., Ma, X., Burkholder, B., Rice, R., Johnson, J. R., Kim, E.-K., et al. (2021). MMS observations of the multiscale wave structures and parallel electron heating in the vicinity of the southern exterior cusp. *Journal of Geophysical Research: Space Physics*, *126*, e2019JA027698. https://doi.org/10.1029/2019JA027698

Onsager, T. G., Grubb, R., Kunches, J., Matheson, L., Speich, D., Zwickl, R., & Sauer, H. (1996). Operational uses of the GOES energetic particle detectors. *In GOES-8 and Beyond*, *2812*, 281–290. Edward R. Washwell.

Opgenoorth, H. J., Oksman, J., Kaila, K. U., Nielsen, E., & Baumjohann, W. (1983). Characteristics of eastward drifting omega bands in the morning sector aurora. *Journal of Geophysical Research*, *88*, 9171–9185. https://doi.org/10.1029/ja088ia11p09171

Opgenoorth, H. J., Persson, M. A. L., Pulkkinen, T. I., & Pellinen, R. J. (1994). Recovery phase of magnetospheric substorms and its association with morning sector aurora. *Journal of Geophysical Research*, *99*, 4115–4129. https://doi.org/10.1029/93JA01502

Partamies, N., Weygand, J. M., & Juusola, L. (2017). Statistical study of auroral omega bands. *Annals of Geophysics*, *35*, 1069–1083. https://doi.org/10.5194/angeo-35-1069-2017

Paxton, L. J., Meng, C.-I., Fountain, G. H., Ogorzalek, B. S., Darlington, E. H., Goldstein, J., et al. (1992a). Special Sensor UV spectrographic imager (SSUSI): An instrument description. In: *Instrumentation for Planetary and Terrestrial Atmospheric Remote sensing*, *1745*, 2–15.

Paxton, L. J., Meng, C.-I., Fountain, G. H., Ogorzalek, B. S., Darlington, E. H., Goldstein, J., & Peacock, K. (1992b). SSUSI: Horizon-to-horizon and limb viewing spectrographic imager for remote sensing of environmental parameters. *Ultraviolet Technol*, *1764*, 161–176.

Peroomian, V., Garg, S., & El-Alaoui, M. (2014). An MHD simulation study of the dynamics of the 8–9 March 2008 CIR-/HSS-driven geomagnetic storm. *Journal of Geophysical Research: Space Physics*, *119*(4), 2990–3001.

Pulkkinen, T. I., Pellinen, R. J., Koskinen, H. E. J., Opgenoorth, H. J., Murphree, J. S., Petrov, V., et al. (1991). Auroral signatures of substorm recovery phase: A case study. *Washington DC American Geophysical Union Geophysical Monograph Series*, *64*, 333–342.

Raeder, J., Walker, R. J., & Ashour-Abdalla, M. (1995). The structure of the distant geomagnetic tail during long periods of northward IMF. *Geophysical Research Letters*, *22*, 349–352. https://doi.org/10.1029/94gl03380

Rostoker, G., & Samson, J. C. (1984). Can substorm expansive phase effects arid low frequency Pc magnetic pulsations be attributed to the same source mechanism? *Geophysical Research Letters*, *11*, 271–274. https://doi.org/10.1029/gl011i003p00271

Roux, A., Perrant, S., Morane, A., Robert, P., Korth, A., Kremser, G., et al. (1991). Plasma sheet instability related to the westward traveling surge. *Journal of Geophysical Research*, *96*(A1017), 697714–697717. https://doi.org/10.1029/91ja01106

Saito, T. (1978). Long period irregular micropulsations, Pi 3. *Space Science Reviews*, *21*, 427. https://doi.org/10.1007/bf00173068

Sigsbee, K., Cattell, C. A., Fairfield, D., Tsuruda, K., & Kokubun, S. (2002). Geotail observations of low-frequency waves and high-speed earthward flows during substorm onsets in the near magnetotail from 10 to 13 RE. *Journal of Geophysical Research*, *107*(A7). https://doi.org/10.1029/2001ja000166

Singer, H. J., Matheson, L., Grubb, R., Newman, A., & Bouwer, S. D. (1996). Monitoring space Weather with the GOES magnetometers. In *GOES-8 and beyond*, (Vol. 2812, pp. 299–308). SPIE Conference Proceedings.

Tagirov, V. (1993). Auroral torches: Results of optical observations. *Journal of Atmospheric and Terrestrial Physics*, *55*, 1775–1787. https://doi.org/10.1016/0021-9169(93)90144-n

Tsyganenko, N. A. (1989). Magnetospheric magnetic field model with a warped current sheet. *Planetary and Space Science*, *37*, 5–20. https://doi.org/10.1016/0032-0633(89)90066-4

Tsyganenko, N. A. (1995). Modeling the Earth's magnetospheric magnetic field confined within a realistic magnetopause. *Journal of Geophysical Research*, *100*(A4), 5599–5612. https://doi.org/10.1029/94ja03193

Tsyganenko, N. A. (1996). *Effects of the solar wind conditions on the global magnetospheric configuration as deduced from data-based field models*. European Space Agency Publication.

Tsyganenko, N. A. (2002a). A model of the near magnetosphere with a dawn-dusk asymmetry—1. Mathematical Structure, *Journal of Geophysical Research*, *107*(A8). https://doi.org/10.1029/2001JA000219

Tsyganenko, N. A. (2002b). A model of the near magnetosphere with a dawn-dusk asymmetry—2. Parameterization and fitting to observations. *Journal of Geophysical Research*, *107*(A7), 10. https://doi.org/10.1029/2001JA000220

Vanhamäki, H., Kauristie, K., Amm, O., Senior, A., Lummerzheim, D., & Milan, S. (2009). Electrodynamics of an omega-band as deduced from optical and magnetometer data. *Annals of Geophysics*, *27*, 3367–3385.

Weygand, J. M., Kivelson, M. G., Frey, F. U., Rodriguez, J. V., Angelopoulos, V., Redmon, R., et al. (2015). An interpretation of spacecraft and ground based observations of multiple omega band events. *Journal of Atmospheric and Solar-Terrestrial Physics*, *133*, 185–204. https://doi.org/10.1016/j.jastp.2015.08.014

Wild, J. A., Woodfield, E. E., Donovan, E., Fear, R. C., Grocott, A., Lester, M., et al. (2011). Midnight sector observations of auroral omega bands. *Journal of Geophysical Research*, *116*, A00I30. https://doi.org/10.1029/2010JA015874

Yamamoto, T. (2008). A linear analysis of the hybrid Kelvin Helmholtz/Rayleigh Taylor instability in an electrostatic magnetosphere-ionosphere coupling system. *Journal of Geophysical Research*, *113*, A06206. https://doi.org/10.1029/2007JA012850

Yamamoto, T., (2009). Hybrid Kelvin-Helmholtz/Rayleigh-Taylor instability in the plasma sheet, *Journal of Geophysical Research*, *114*, A06207. https://doi.org/10.1029/2008JA013760

Yamamoto, T. (2011). A numerical simulation for the omega band formation. *Journal of Geophysical Research*, *116*, A02207. https://doi.org/10.1029/2010JA015935

Yamamoto, T., Inoue, S., & Meng, C. I. (1997). Formation of auroral omega bands in the paired region 1 and region 2 field aligned current system. *Journal of Geophysical Research*, *102*(A2), 2531–2544. https://doi.org/10.1029/96ja02456

Yamamoto, T., Makita, K., Ozaki, M., & Meng, C.-I. (1993). A particle simulation of auroral omega bands and torch-like structures. *Journal of Geomagnetism and Geoelectricity*, *45*, 619–648. https://doi.org/10.5636/jgg.45.619